Available online at www.sciencedirect.com
ScienceDirect
Mendeleev Commun., 2015, **25**, 174–176
Mendeleev Communications

Novel supramolecular system based on a cationic amphiphile bearing glucamine fragment: structural behavior and hydrophobic probe binding

Dinar R. Gabdrakhmanov,[a,b] Farida G. Valeeva,[a,b] Victor V. Syakaev,[a] Svetlana S. Lukashenko,[a,b] Sergey V. Zakharov,[b] Dmitry A. Kuryashov,[b] Natalia Yu. Bashkirtseva,[b] Lucia Ya. Zakharova,*[a,b] Shamil K. Latypov[a] and Oleg G. Sinyashin[a,b]

[a] *A. E. Arbuzov Institute of Organic and Physical Chemistry, Kazan Scientific Center of the Russian Academy of Sciences, 420088 Kazan, Russian Federation. Fax: +7 843 273 2253; e-mail: lucia@iopc.ru*
[b] *Kazan National Research Technological University, 420015 Kazan, Russian Federation*

DOI: 10.1016/j.mencom.2015.05.004

The synthesized cationic surfactant bearing a glucamine fragment forms spherical micelles at about 0.7 mmol dm^{-3} and displays specific aggregation characterized by a sharp growth of micelles and a change in their properties within a narrow concentration range about 10 mmol dm^{-3}.

Amphiphilic compounds are of special interest as drug and gene delivery systems.[1,2] Cationic surfactants exhibit high affinity toward negatively charged biospecies, such as DNA, and they are used as effective transfectants.[3,4] Drug carriers should be characterized by nanosized dimensions, biocompatibility, low toxicity, high loading capacity, *etc*. Based on these criteria, special attention is paid to cationic surfactants bearing natural fragments.[4–6] In our work, this trend is taken into account.[7–11]

Sugar-based compounds including glucamine and its hydrophobized derivatives are of interest due to complexation, water purification and self-assembly properties.[4–6,12–14] The majority of investigated surfactants have the bromide counterion, whereas the counterions markedly affect the properties of micelles including critical micelle concentration (cmc), aggregation numbers and the size and morphology of aggregates.[15,16] The effect of the counterion is determined by the Hofmeister series: F < Cl < Br < I. The iodide ion exhibits a maximum effect among inorganic anions and exceeds that of double-charged anions, *e.g.* sulfate ions. Probably, this is owing to the ability of iodide ions to form contact ion pairs with surface active ions,[17] which results in a partial desolvation of head groups allowing for a more compact packing of surfactant molecules. Here, we synthesized a cationic surfactant **1** with iodide counterion bearing a glucamine fragment and studied its self-assembly.†

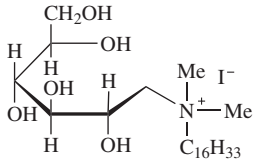

1

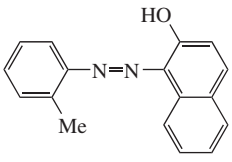

Orange OT

Figure 1 shows tensiometry data, with the breakpoint in the surface tension isotherm corresponding to cmc of 0.73 mmol dm^{-3}. This is slightly lower than the aggregation threshold of cationic surfactants with charged nitrogen head groups and cetyl tails,[21]

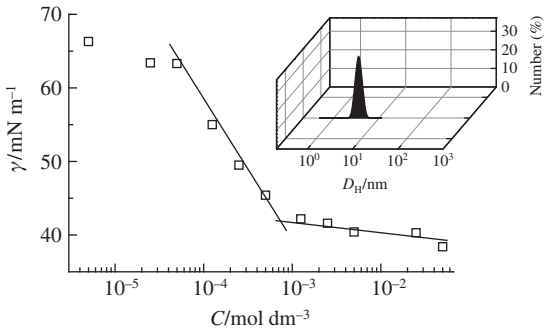

Figure 1 Surface tension isotherm for an aqueous solution of **1**. Inset: DLS data for an aqueous solution of **1** (3 mmol dm^{-3}) in terms of the number averaged size distribution; 30 °C.

† Compound **1** was synthesized by the reaction of *N*-hexadecyl-*N*-methyl-D-glucamine (0.01 mol) with methyl iodide (0.03 mol) in acetonitrile (60 ml) upon boiling for 3 h. After cooling, the precipitate was filtered off, recrystallized from an acetone–methanol mixture and dried *in vacuo*. The yield was 4.2 g (79%), mp 96–98 °C. ^{1}H NMR (DMSO-d_6, 600 MHz) δ: 0.85 (t, 3H, *J* 7.0 Hz, Me), 1.24 (m, 26H, CH_2), 1.68 (m, 2H, CH_2), 3.05 (s, 6H, N^+Me_2), 3.30 (m, 2H, N^+CH_2), 3.34 and 3.48 (m, 2H, N^+CH_2), 3.41 and 3.60 (m, 2H, CH_2OH), 3.49, 3.52, 3.69, 4.09 (m, 4H, CHO), 4.40 (t, 1H, OH, *J* 5.6 Hz), 4.43 (d, 1H, OH, *J* 7.3 Hz), 4.53 (d, 1H, OH, *J* 5.2 Hz), 4.78 (d, 1H, OH, *J* 6.3 Hz), 5.24 (d, 1H, OH, *J* 4.9 Hz). ^{13}C NMR (DMSO-d_6, 151 MHz) δ: 13.8, 21.7, 22.0, 25.7, 28.4, 28.6, 28.7, 28.8, 28.9, 31.2, 50.9, 51.1, 63.3, 64.1, 65.8, 67.1, 70.0, 70.3, 71.3. IR (KBr, ν/cm^{-1}): 3449, 3376, 3286, 2917, 2850, 1468, 1409, 1189, 1141, 1086, 1057, 1036, 852, 723. MS (MALDI), *m*/*z*: 434 [M–I]$^+$. Found (%): C, 51.46; H, 9.85; N, 2.41; I, 22.18. Calc. for $C_{24}H_{52}NO_5I$ (%): C, 51.33; H, 9.33; N, 2.49; I, 22.59. The precursor reagent *N*-hexadecyl-*N*-methyl-D-glucamine was obtained by the reaction of *N*-methylglucamine (Sigma) and hexadecyl bromide (Sigma) in ethanol at a molar ratio of 1 : 1.2.

Water purified with a Milli-Q Water Purification System was used for sample preparation. Commercially available Orange OT and pyrene (Sigma-Aldrich, 95%) were used as hydrophobic probes in the solubilization and fluorescence studies. Aggregation was studied by tensiometry (Krüss K06 tensiometer)[18] and fluorescence ratiometry.[9,19] NMR self-diffusion (Bruker AVANCE-600 spectrometer)[8,11,20] measurements were used to analyze self-assembly. Experimental data were treated in terms of a two-site bound-free model that assumes a fast exchange in the NMR time scale between surfactants in the micelles and in the bulk phase. The exchange-averaged diffusion coefficient is $D_S = D_{mic}P_{mic} + D_{free}(1 - P_{mic})$, where P_{mic} is the fraction of micellized surfactant molecules, D_{mic} is the diffusion coefficient of the micelle, and D_{free} is the diffusion coefficient of the monomer surfactant in the aqueous phase. The hydrodynamic diameter of aggregates was monitored by dynamic light scattering (Malvern Instrument Zetasizer Nano).[7] Viscosity measurements were performed on a HAAKE Rheostress 6000 rheometer (Germany). To examine the solubilization capacity of surfactants, UV-VIS absorption spectra were recorded with a Specord PLUS (Analytik Jena) at 495 nm (absorption maximum of Orange OT).[10]

Table 1 The values of cmc, maximum surface excess (Γ_{max}) and area per surfactant molecule (A_{min}) calculated on the basis of tensiometric data (Figure 1) and solubilization power *S* calculated based on a dye solubilization study (Figure 5) for **1**.[a]

cmc/ mmol dm^{-3}	Γ_{max} /10^6 mol m^{-2}	A_{min}/nm^2	*S*	
			section *1* of the plot	section *2* of the plot
0.73	1.58	1.05	0.0237	0.0131

[a]The surface excess Γ_{max} was calculated using the Gibbs equation

$$\Gamma_{max} = \frac{1}{2.3nRT} \lim_{C \to cmc} (d\pi/d \log C),$$

where *R* is the gas constant, π is the surface pressure obtained from the surface tension of water minus the surface tension of the surfactant solution, *T* is the absolute temperature; *n* is the number of species at the interface, the concentration of which changes with surfactant concentration: $n = 2$ for an ionic surfactant with univalent surfactant ion and counterion; the surface area per molecule $A_{min} = 10^{18}/(N_A\Gamma_{max})$, N_A is the Avogadro number.

which is probably due to the iodide counterion with high affinity toward a micellar pseudophase.[15–17] Quantitative analysis of the surface tension isotherm provides the surface excess and minimal surface area (Table 1). For calculations, the equation of Gibbs adsorption isotherm (see Table 1) was used for the surface active 1-1 electrolytes. Note that a large value of A_{min} was observed in the case of **1**, as compared to the typical cationic surfactant cetyl trimethylammonium bromide (CTAB) (A_{min} ~ 0.5 nm^2 for CTAB[22]). This argues that surfactant **1** tends to form spherical aggregates with a non-compact packing mode.

The self-assembly of compound **1** was strongly supported by the NMR self-diffusion data (Figure 2). The self-diffusion coefficient (D_S) decreased with surfactant concentration. A breakpoint at 0.7 mmol dm^{-3} determined from the D_S *vs.* $1/C_1$ plot agrees well with tensiometry cmc values. Aggregates existing beyond cmc are characterized by a hydrodynamic diameter of 5 to 6 nm (Figure 1, inset), which is in line with spherical micelles and the above calculations of surface area per a molecule (Table 1). At the same time, rough estimation of the aggregation numbers from the self-diffusion coefficients based on the Connolly Solvent-Excluded Volumes (CSEV)[11,23] showed a sharp increase in the aggregation number within a concentration range of 5–10 mmol dm^{-3}. This allows us to assume that changes in the structure or shape of aggregates[21] probably occur within this concentration range. To test the assumption we carried out viscosity measurements and a fluorescence ratiometry study. Both of these parameters reflect the properties of a microenvironment sensitive to the structure of aggregates. As can be seen, the viscosity *vs.* concentration plot undergoes changes within a similar concentration range at ⩾ 10 mmol dm^{-3} (Figure 3, inset) to confirm the above assumption. Note that the concentrations corresponding to the structural rearrangements strongly depend on the method used; therefore, this is generally followed by some discrepancy in cmc[24] or critical concentration values corresponding to structural transitions.[25,26]

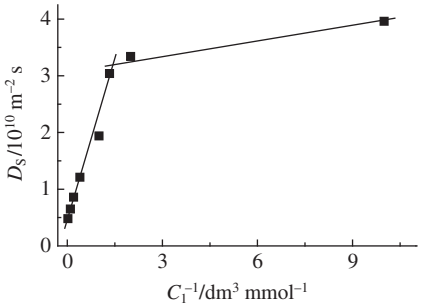

Figure 2 Self-diffusion coefficient (D_S) as a function of concentration for **1** in D_2O; NMR self-diffusion technique; 30 °C.

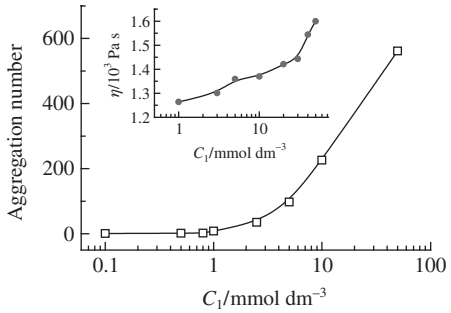

Figure 3 Aggregation number *vs.* surfactant concentration plot for the solutions of **1** in D_2O, 30 °C. Inset: the concentration dependence of the viscosity of **1** at 25 °C.

Since the geometry of a head group favors the spherical micelle formation, one can assume that the iodide counterion is responsible for the observed changes in the properties of aggregated **1** at a surfactant concentration of around 10 mmol dm^{-3}. It should be clarified that, while the change in viscosity is quite obvious, it is rather small to assume the formation of long worm-like micelles. The sphere-to-rod transition is documented to occur at 250–300 mmol dm^{-3} for CTAB and at 15–20 mmol dm^{-3} for the tosylate analogue CTAT.[27] Although the iodide counterion shows a superior effect, as compared to that of inorganic anions,[15,16] it is unlikely that it would be higher than the influence of a hydrotrope organic anion. Therefore, the above structural changes can reflect the structural rearrangement of spherical micelles to elongated spheroidal aggregates with a more compact packing of molecules. Importantly, the viscosity behavior of drug delivery formulations is a key factor controlling the release of loaded drugs.[28]

One of the most informative and sensitive methods for the examination of self-assembly is a fluorescence probe technique with pyrene used as a probe.[19] In particular, the fluorescence intensity ratio between the first peak at 373 nm (I_1) and the third peak at 384 nm (I_3) in the spectrum of pyrene is very sensitive to the micropolarity of the probe. Therefore, the I_1/I_3 ratio is often used to determine cmc. Figure 4 testifies micelle formation with cmc coinciding with that determined by other techniques. Meanwhile, with an increase in the concentration around 10 mmol dm^{-3}, the dependence markedly changes, which reflects changes in the structure of aggregates revealed from data on their aggregation numbers and viscosity (Figure 3). Similar changes in the shape and properties of aggregates were detected by calorimetry for cationic micelles with ammonium head groups including CTAB.[29] This phenomenon was attributed to changes in water structure in solvate shells, resulting in a partial desolvation of head groups and micellar growth.

Arguments in favor of micelle formation and changes in their structure and properties are provided by dye solubilization

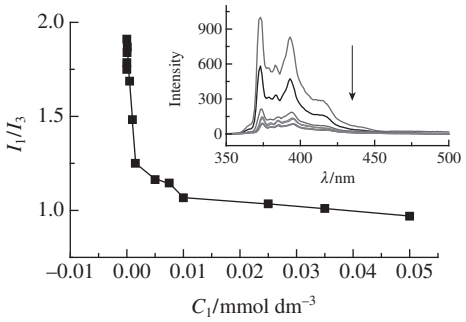

Figure 4 Ratio between pyrene fluorescence intensities at the first (373 nm) and third (384 nm) vibronic peaks as a function of concentration of **1** at 25 °C. Inset: pyrene fluorescence spectra (the arrow indicates an increase in the concentration of surfactant **1**); 25 °C.

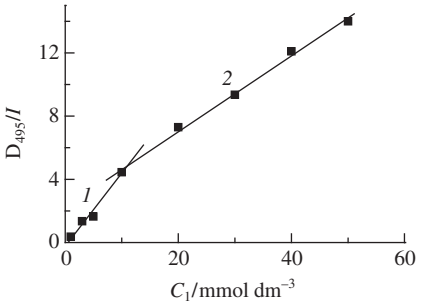

Figure 5 Reduced absorbance of Orange OT at 495 nm (re-calculated for an optical path length of 1 cm) *vs.* concentration of **1**; 25 °C.

(Figure 5). Orange OT is a hydrophobic probe completely insoluble in water; therefore, it shows no absorbance at 495 nm without a surfactant. The addition of surfactants results in the appearance of absorbance at 495 nm due to encapsulation of the dye by the nonpolar core of direct micelles. On the one hand, this indicates the onset of aggregation, while, on the other, it characterizes the potentiality of aggregates to be used as nanocontainers. The cmc value determined as the cross-points of linear portions of the dependences with the *x* axis is 0.65 mmol dm^{-3}. The slope of a linear part (Table 1) characterizes the solubilization power (*S*) of aggregates toward Orange OT, *i.e.*, the number of solubilized dye molecules per mole of aggregated surfactants. It is $S = b/\varepsilon$, where *b* is the slope of the D_{495} *vs. C* plot (Figure 5), and ε is the extinction coefficient of the dye (17 400 dm^3 mol^{-1} cm^{-1}). According to Figure 5 and Table 1, the dependence for **1** consists of two sections with solubilization powers of 0.0237 and 0.0131 dm^3 mol^{-1} cm^{-1}, respectively. Apparently, two different types of aggregates correspond to these concentration ranges with a threshold around 10 mmol dm^{-3}. This strongly supports the above data indicating the structural transition of aggregates between 5 and 10 mmol dm^{-3}. Importantly that while somewhat decrease in *S* occurs beyond breakpoint, the solubilization capacity of aggregated **1** around cmc exceeds that of CTAB.[30] This provides evidence for a rather high potentiality of **1** as nanocontainer for hydrophobic species. The specific aggregation behavior of compound **1** that is displayed in a markedly fast growth of micelles and is followed by sharp changes in their properties, especially solubilization capacity can be used for control of the binding-release of guest molecules.

This work was supported by the Russian Science Foundation (grant no. 14-23-00073).

References

1 M. S. Dzyurkevich, K. N. Timofeeva, D. A. Faizullin, Yu. F. Zuev, I. I. Stoikov and V. V. Plemenkov, *Mendeleev Commun*., 2014, **24**, 224.
2 A. V. Galukhin and I. I. Stoikov, *Mendeleev Commun*., 2014, **24**, 82.
3 S. Gaweda, M. Carmen Moran, A. A. C. C. Pais, R. S. Dias, K. Schillen, B. Lindman and M. Graca Miguel, *J. Colloid Interface Sci*., 2008, **323**, 75.
4 Y. Li, X. Zhang, Y. Li, C. Li and X. Guo, *Colloids Surf. A*, 2014, **443**, 224.
5 *Sugar-Based Surfactants: Fundamentals and Applications*, ed. C. C. Ruiz, CRC Press, Boca Raton, 2009, p. 640.
6 O. O. Koloskova, U. A. Budanova, A. M. Sumina, G. A. Sarychev and Yu. L. Sebyakin, *Mendeleev Commun*., 2014, **24**, 262.
7 L. Zakharova, M. Voronin, V. Semenov, D. Gabdrakhmanov, V. Syakaev, Yu. Gogolev, R. Giniyatullin, S. Lukashenko, V. Reznik, Sh. Latypov, A. Konovalov and Yu. Zuev, *ChemPhysChem*, 2012, **13**, 788.
8 S. V. Kharlamov, M. A. Voronin, V. E. Semenov, D. R. Gabdrakhmanov, A. E. Nikolaev, V. S. Reznik, L. Ya. Zakharova and A. I. Konovalov, *Colloids Surf. B*, 2013, **111**, 218.
9 D. R. Gabdrakhmanov, M. A. Voronin, L. Ya. Zakharova, A. I. Konovalov, R. N. Khaybullin, I. Yu. Strobykina, V. E. Kataev, D. A. Faizullin, N. E. Gogoleva, T. A. Konnova, V. V. Salnikov and Yu. F. Zuev, *Phys. Chem. Chem. Phys*., 2013, **15**, 16725.
10 M. A. Voronin, D. R. Gabdrakhmanov, R. N. Khaibullin, I. Yu. Strobykina, V. E. Kataev, B. Z. Idiyatullin, D. A. Faizullin, Yu. F. Zuev, L. Ya. Zakharova and A. I. Konovalov, *J. Colloid Interface Sci.*, 2013, **405**, 125.
11 L. Ya. Zakharova, V. E. Semenov, V. V. Syakaev, M. A. Voronin, D. R. Gabdrakhmanov, F. G. Valeeva, A. S. Mikhailov, A. D. Voloshina, V. S. Reznik, Sh. K. Latypov and A. I. Konovalov, *Mater. Sci. Eng., C*, 2014, **38**, 143.
12 L. Toledo, B. L. Rivas, B. F. Urbano and J. Sánchez, *Sep. Purif. Technol.*, 2013, **103**, 1.
13 A. Sabarudin, K. Oshita, M. Oshima and Sh. Motomizu, *Talanta*, 2005, **66**, 136.
14 S. Warwel, F. Brüse and H. Schier, *J. Surfact. Deterg.*, 2004, **7**, 181.
15 P. L. Nostro and B. W. Ninham, *Chem. Rev*., 2012, **112**, 2286.
16 S. Nihonyanagi, S. Yamaguchi and T. Tahara, *J. Am. Chem. Soc*., 2014, **136**, 6155.
17 M. N. Islam, K. C. Sarker and K. K. Sharker, *J. Surfact. Deterg*., 2015, **18**, 9.
18 L. Zakharova, F. Valeeva, A. Zakharov, A. Ibragimova, L. Kudryavtseva and H. Harlampidi, *J. Colloid Interface Sci*., 2003, **263**, 597.
19 K. Kalyanasundaran and J. K. Thomas, *J. Am. Chem. Soc*., 1977, **99**, 2039.
20 D. Wu, A. Chen and C. S. Johnson, *J. Magn. Reson., Ser. A*, 1995, **115**, 260.
21 *Surfactants and Polymers in Aqueous Solution*, 2nd edn., eds. K. Holmberg, B. Jonsson, B. Kronberg and B. Lindman, John Wiley & Sons, Chichester, 2003, p. 562.
22 F. Jalali, M. Shamsipur and N. Alizadeh, *J. Chem. Thermodyn*., 2000, **32**, 755.
23 M. L. Connolly, *J. Am. Chem. Soc*., 1985, **107**, 1118.
24 A. Zdziennicka, K. Szymczyk, J. Krawczyk and B. Janczuk, *Fluid Phase Equilib*., 2012, **322–323**, 126.
25 P. A. Hassan and J. V. Yakhmi, *Langmuir*, 2000, **16**, 7187.
26 K. Kuperkar, L. Abezgauz, D. Danino, G. Verma, P. A. Hassan, V. K. Aswal, D. Varade and P. Bahadur, *J. Colloid Interface Sci.*, 2008, **323**, 403.
27 C. Gamboa, H. Rios and L. Sepulveda, *J. Phys. Chem.*, 1989, **93**, 5540.
28 L. Starýchová, M. Žabka, M. Špaglová, M. Čuchorová, M. Vitková, M. Čierna, K. Bartoníková and K. Gardavská, *J. Pharm. Sci*., 2014, **103**, 3977.
29 M. J. Blandamer, B. Briggs, J. Burgess, P. M. Cullis and G. Eaton, *J. Chem. Soc., Faraday Trans*., 1991, **87**, 1169.
30 G. A. Gainanova, G. I. Vagapova, A. R. Ibragimova, F. G. Valeeva, V. V. Syakaev, E. V. Tudriy, I. V. Galkina, O. N. Kataeva, L. Ya. Zakharova, Sh. K. Latypov and A. I. Konovalov, *J. Colloid Interface Sci.*, 2012, **367**, 327.

Received: 28th October 2014; Com. 14/4496